Atomic Oxygen Effects on Hyperbranched Polysiloxane Polyimides in Ground–Based Simulated Low Earth Orbit Environments

Xingfeng Lei（雷星锋）, Mingtao Qiao，　Pan Yao, Lidong Tian, Qiuyiu Zhang* （张秋禹）

Department of Applied Chemistry, School of Science, Northwestern Polytechnical University（西北工业大学理学院应用化学系）, Xi'an, 710072, P. R. China.

Abstract: Here, we report for the first time the fabrication of novel hyperbranched polysiloxane (HBPSi) polyimides by co–polymerizing common imide monomers with amine–functionalized HBPSi in solution and thermal imidization. Resulting hybrid membranes exhibited a combination of desirable properties, in particular high AO resistance. The AO resistance of the membranes were evaluated based on their mass loss, surface morphology and AO erosion yield. Results indicated that the AO erosion yield of the resulting hybrid membranes decreased with increasing both HBPSi amount and AO fluence. Surface morphologies suggest that a dense and connected silica passivating layer plays a more positive role in resisting AO attack and the passivating layer grows with AO fluence and becomes increasingly resistant to AO attack. After irradiation to AO fluence of ca. 3.87×10^{20} O atoms·cm^{-2}, 29.7 wt % HBPSi polyimide demonstrated the mass loss as little as 5.9% that of pristine polyimide. The whole development of the HBPSi polyimides is low cost, environmentally friendly and easy to operate, which is suitable for mass production. This promises that this newly–developed material may find wide usefulness as protective materials onboard spacecrafts to resist AO attack in space applications.

Keywords: low earth orbit (LEO), polyimide, atomic oxygen (AO), hyperbranched polysiloxane, polymer degradation

1. Introduction

Polyimides, in particular aromatic polyimides like Kapton® H, are extensively used onboard spacecrafts mainly as lightweight flexible substrates, surface protective materials and thermal control materials, [1-16] owing to its inherent strong mechanical strength, high–temperature stability, desirable chemical resistance and good UV radiation stability [17-20]. So far, there are no commercially available polyimides inherently withstanding atomic oxygen (AO) attack, which is present in the low earth orbit (LEO). In order to improve the AO resistance of polyimides, coating technology is often used and some inorganic coatings such as aluminum (or gold or germanium) are typically coated onto Kapton® H to resist AO attack [3,10,21]. However, such protective coatings must have enough reliability and extremely low defects to maintain its performance during missions, since coating degradation, spalling, cracking, or disbonding will cause severe erosion to the underlying polymers [12]. Furthermore, most inorganic coatings are inflexible and very fragile, which necessitates special care during assembly and stowage, and thus raising the production cost [12,21,22]. Therefore, rational molecular design focusing on the molecular skeleton modification of polymeric materials, other than coating technology, is the key to manufacture new polyimides with desirable AO resistance.

One effective strategy is to introduce siloxane units into polyimide molecular chains by copolymerizing imide monomers with siloxane units to fabricate AO–resistant polyimides [6,12,23-29], for silicon–oxygen bonding energy is about 8 eV, a little higher than AO translational energy, and this bond seems intact and impervious upon AO exposure [6,12,23]. Among a few examples of siloxane–containing polyimides, those fabricated with polyhedral oligomeric silsesquioxane (POSS) have drawn great attention in the past several years, owing to the flexible tailorability of POSS monomers [6,23-25,30]. When exposed to AO, POSS polyimides are likely to

form a silica passivating layer on the surface and hence prevents the underlying polymer from additional erosion [6,23,24]. However, it is significant to note that, the previously reported work typically involving POSS monomer looks specifically at bifunctional POSS–diamines, which are relatively expensive and difficult to synthesize. Generally, POSS–diamine synthesis involves such expensive starting monomers as octa–cyclopentyl POSS and (aminopropyl)–hepta–isobutyl POSS *etc.*, and the whole synthetic process is relatively high–cost and difficult to operate [6], which limits the commercial use of POSS polyimides, in particular mass production. Octa–functional POSS, such as octa–(aminopropyl or aminophenyl)silsesquioxane (OAPS), in contrast, is easy to manufacture and not that expensive in comparison to POSS–diamine [30,31], but it is difficult to get all of the amine groups reacted and hence one could not make polymers with well–defined structures. In addition, insoluble gels usually form within several minutes immediately the OAPS is added to the polyamic acid solutions, and thus polyimide membranes could not be obtained [31]. In addition to POSS polyimide block–copolymers, Tagawa and co–workers has also investigated the AO degradation characteristic of a commercially available Si–containing polyimide (BSF30) [27]. Although the erosion yield of BSF30 reached as low as 4% that of the standard PMDA–ODA polyimide, BSF30 exhibited poor tensile strength (about 61 MPa), low glass transition temperature (T_g = ca. 175 °C) and remarkable coefficient of thermal expansion (CTE = ca. 136 ppm/K), which might not meet the space requirements.

Considering the capital cost and large–scale production, our group has recently designed and prepared several kinds of amine–functionalized hyperbranched polysiloxanes (HBPSis) through a facile method, which has been copolymerized with imide monomers to fabricate high–performance polyimides [28]. However, in consideration of the industrial demand of AO resistance of polyimide

membranes, further efforts are still needed to fabricate a highly AO survivable polyimide membranes.

Here, we report for the first time the synthesis of a novel amine–functionalized HBPSi by adopting tetraethoxysilane (TEOS), γ–aminopropyltriethoxysilane (APS) and diphenyldimethoxysilane (DPMS), to give an inorganic/organic hybrid three–dimensional compact structure according to scheme 1. These siloxanes were chosen because they are common reagents and commercially available. In addition, the hydrolysate of TEOS has the similar structure to SiO_2, which is expected to impart high silicon content as well as high O/Si ratio to finally formed HBPSi macromonomers, for silicon–containing units with high O/Si ratio and high oxidation states are favorable to improve the AO resistance of hybrid polyimides [28,29]. Additionally, DPMS possesses two phenyl groups, much more stable than other organic substituents. Hence we expect this well–designed HBPSi macromonomer may contribute significantly enhanced AO resistance and desirable thermal stability to resulting polyimides.

In this paper, the resistance of the resulting membranes to AO attack were thoroughly investigated in a simulated LEO environment and the AO resistance were evaluated based on their mass loss, surface morphology and AO erosion yield. Besides, the relationship between the erosion yields of resulting HBPSi polyimides and their structures is also discussed herein. These evaluations may contribute some effective viewpoints to the erosion/protection mechanism and degradation behavior of HBPSi polyimides in simulated AO environment for LEO.

2. Experimental section

2.1 Materials

Tetraethoxysilane (TEOS), γ–aminopropyltriethoxysilane (APS) and diphenyldimethoxysilane

(DPMS) were purchased from Nanjing Chengong silicon co., Ltd (Nanjing, China) and used as received. 4,4'–Diaminodiphenyl ether (ODA) and pyromellitic dianhydride (PMDA) were provided by Sinopharm Chemical Reagent Co. Ltd (Beijing, China) and purified by vacuum sublimation prior to use. *N,N′*–Dimethylacetamide (DMAc) was purchased from Tianjin Fuyu Fine Chemicals Co. Ltd (Tianjin, China) and purified by distillation under reduced pressure over phosphorus pentoxide and stored over 4 Å molecular sieves prior to use.

2.2 General characterization

The molecular structure parameters of HBPSi were determined on a DAWN EOS size exclusion chromatography/multiangle laser light scattering (SEC/MALLS) instrument equipped with a highly cross–linked styrene/divinylbenzene gel columns (500 Å, 5 μm) and a viscometer (Wyatt Technology). Fourier transform infrared (FT–IR) spectra were determined with a FT–IR spectrometer (BRUKER TENSOR 27). Inherent viscosities (η_{inh}) were obtained on 0.5% (w/v) polyamic acid (PAA) solutions in freshly distilled *N,N′*–dimethylacetamide (DMAc) at 25 °C with an Ubbelohde viscometer.

2.3 AO exposure testing

Ground–based AO exposure measurements were performed with a combined space effects testing facility (CSETF) equipped with neutral AO beam and vacuum ultraviolet ray (VUV) sources. The specific operation procedures and details of the system were described in our previous studies [28,29]. The cross–section view of low–energy neutral beam facility was shown in figure 1. The AO flux at the sample's position was finally calibrated to be approximately 4.89×10^{15} atom·cm^{-2}·s^{-1}.
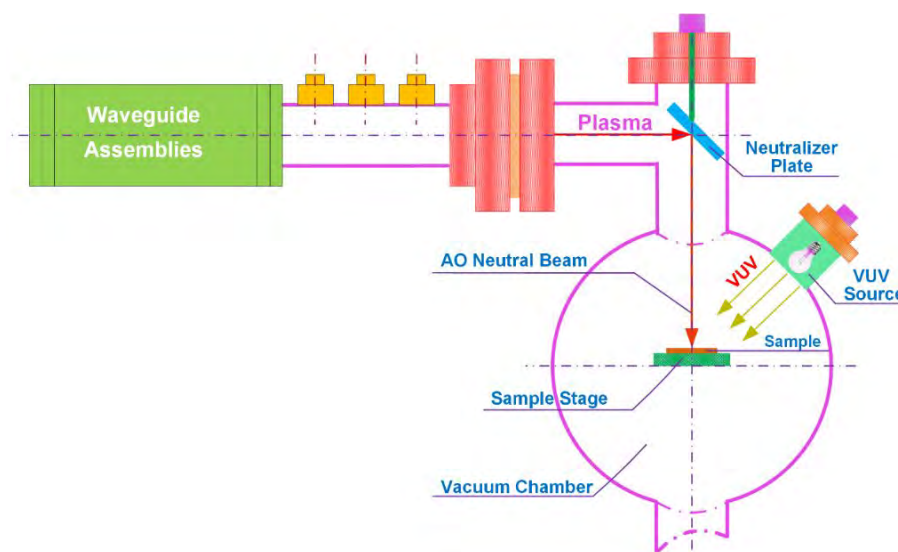
Figure 1. Cross–section view of low–energy neutral beam facility configured for AO exposure measurements.

2.4 Surface characterization

Surface morphologies of polyimide membranes before and after AO exposure were observed with a Scanning Electron Microscope (SEM, JEOL JSM–6700F). The elemental compositions and variations of the electron state of surface elements before and after AO exposure were analysed on an AXIS Ultra DLD X–Ray Photoelectron Spectroscopy (XPS) instrument (Kratos Co., UK) equipped with a monochromatic Al Kα X–Ray source with a residual pressure of ca. 10^{-8} Pa. The pass energy during the whole measurement was 40 eV. The shifts of binding energy of XPS curves were corrected by assuming that the lowest C1s component was 284.6 eV for the unexposed polyimide (0 wt %

HBPSi) sample.

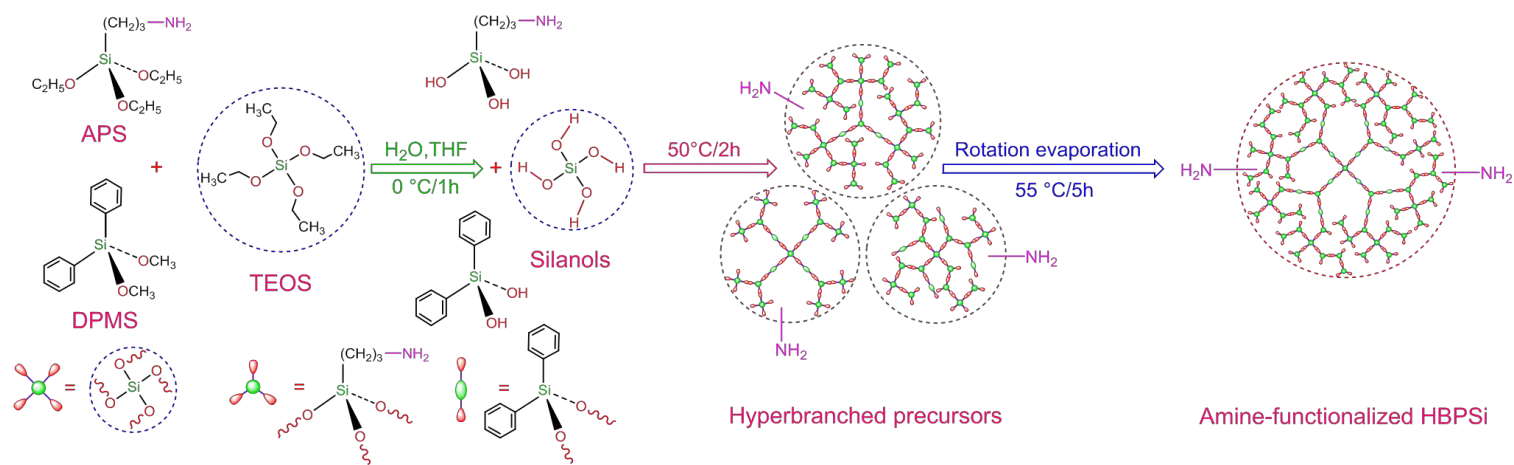2.5 Synthesis of amine–functionalized hyperbranched polysiloxane (HBPSi) macromonomer

Amine–functionalized HBPSi macromonomer was synthesized by reacting tetraethoxysilane (TEOS), γ–aminopropyltriethoxysilane (APS) and diphenyldimethoxysilane (DPMS) in the presence of H_2O in HPLC grade tetrahydrofuran (THF). Typically, to a 100 mL, round–bottom flask containing 25 g of THF was added 0.01 mol of TEOS, 0.07 mol of DPMS and 6.5 mmol of APS. After the reaction mixture was chilled to 0 °C in an ice bath, 2.565 g (14.25 mmol) of deionized water was added dropwise through a syringe under vigorous stirring over a period of 0.5 h. The reaction mixture was stirred at 0 °C for 1 h and afterward for an additional 2 h at 50 °C. After 5 h's rotary evaporation under a reduced pressure at 55 °C, a white powder product with 0.47 mmol/g of amine content was obtained. The synthetic procedure of amine–functionalized HBPSi was shown in scheme 1.

Table 1. Recipe for the synthesis of pristine and HBPSi polyamic acids.

Sample	ODA/g	PMDA/g	HBPSi/g	DMAc/g
Pristine PI	2.00	2.18	—	30.65
4.1 wt % HBPSi–PI	1.99	2.18	0.18	31.90
8.8 wt % HBPSi–PI	1.98	2.18	0.40	33.44
14.4 wt % HBPSi–PI	1.97	2.18	0.70	35.56
21.9 wt % HBPSi–PI	1.95	2.18	1.16	38.79
29.7 wt % HBPSi–PI	1.92	2.18	1.73	42.75

2.6 Preparation of HBPSi polyimide (HBPSi–PI) membranes

Hybrid membranes were prepared as depicted in scheme 2. Polyamic acids (PAAs) from ODA and PMDA with different HBPSi addition, varied between 4.1 wt % and 29.7 wt % were prepared according to table 1 as 12 wt % solid content of PAA in freshly distilled DMAc in all cases. A representative procedure for 8.8 wt % HBPSi PAA precursor is as follows. Specifically, amine–functionalized HBPSi (0.40 g) and ODA (1.98 g, 9.905 mmol) were added into an absolutely dry, round bottom flask charged with 36 mL of freshly distilled DMAc with stirring under nitrogen purge. After ODA and HBPSi were completely dissolved, PMDA (2.18 g, 10 mmol) was quickly added in one portion and reacted at room temperature under nitrogen atmosphere for 24 h to afford a viscous PAA solution. The membrane fabrication was carried out by casting corresponding PAA solutions onto dust–free glass plates by using an adjustable doctor blade. Thermal imidization (4 °C/min, 360 °C/1 h) is adopted herein to yield fully imidized membranes. Resulting membranes were finally obtained by peeling off from the glass plates and afterward dried in a vacuum oven at 120 °C for 4 h.

Scheme 1. Possible chemical structure of amine–functionalized HBPSi macromonomer and its synthesis route through hydrolytic co–condensations of siloxane compounds.
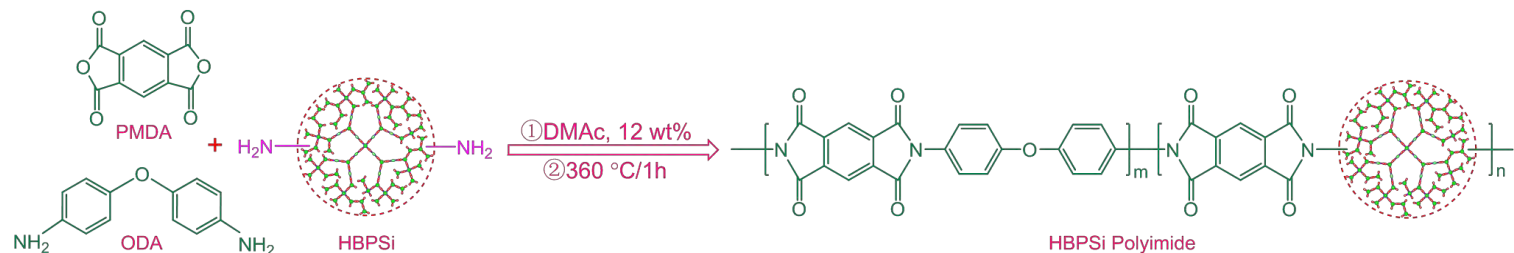
Scheme 2. Fabrication of HBPSi polyimide membranes through copolycondensation and thermal imidization. Note: The molecular structure of HBPSi polyimide presented here represents one of the possible molecular structures.

Table 2. Main molecular conformation parameters of amine–functionalized HBPSi macromonomer.

Sample	$M_n{}^a$ (g/mol)	$M_w{}^a$ (g/mol)	$M_w/M_n{}^a$	$R_{h(n)}{}^a$ (nm)	$\eta_n{}^a$ (mL/g)	α^a	K^a (mL/g)	dn/dc^b (mL/g)
HBPSi	3826	5173	1.352	0.7	5.0	0.39	0.206	0.158

^{a} Determined by SEC/MALLS equipped with a viscometer. ^{b} Determined in THF by an Optilab rEX detector at 25 °C through a batch model.

3. Results and discussion

3.1 HBPSi synthesis and membrane formation

The synthesis of amine–functionalized HBPSi macromonomer typically involves three steps as shown in scheme 1. The starting monomers, TEOS, APS and DPMS were first hydrolyzed in dilute THF solution at low temperature to give silanols and subsequently converted to HBPSi precursors via condensation reactions at 50 °C. Finally, the precursors were further condensed with concurrently removal of undesirable volatiles by vacuum rotation evaporation to afford the final HBPSi macromonomer. The HBPSi synthesis was affected by many factors such as water addition, water mole ratio, addition of catalyst, reaction time and temperature [33-38]. Among which, water addition is the most significant effect. During hydrolytic process, water should be added so slowly that the water concentration approached zero to avoid any high local concentration. Once water were directly added or even if the addition of water was not slow enough, gelation occurred immediately [33-36].

HBPSi polyimides with various proportions of HBPSi were synthesized by co–polymerizing HBPSi with ODA and PMDA in a polar aprotic solvent. To obtain high–molecular–weight polyimides, the molar ratio of amine groups to anhydride groups was strictly controlled at 1:1 in all cases. The membrane preparation involves two steps. Firstly, polyamic acids were synthesized according to the formulations summarized in table 1 and secondly, the precursors were thermal–treated to yield fully imidized polyimide membranes. No gelation occurred during polymerization which was attributed to the desirable amine content on each HBPSi molecule, and this would make it easier to prepare HBPSi polyimides in a large scale.

3.2 Structure analysis

3.2.1 FT–IR spectrum of amine–functionalized HBPSi

Figure 2 shows the FT–IR spectrum of amine–functionalized HBPSi. The characteristic primary amine bands at 3480 and 3418 cm^{-1} imply the HBPSi macromonomer has been successfully functionalized with amine groups. The spectrum also contains bands ascribed to phenyl group, 3058 and 3011 cm^{-1} (C–H stretching) and aminopropyl group, 2922 and 2853 cm^{-1} (C–H stretching) [39,40]. The intense absorptions between 1090 and 1120 cm^{-1} ascribed to Si–O–Si stretching, confirms the presence of Si–O–Si network in HBPSi molecules [28,39].
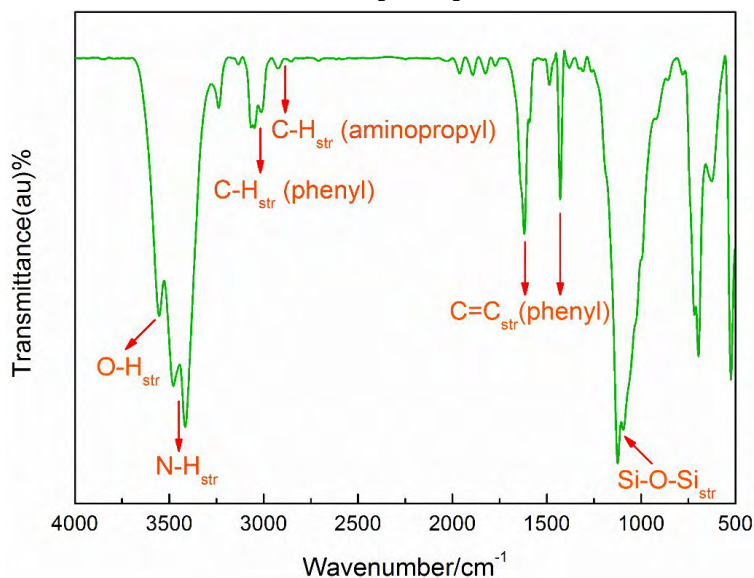
Figure 2. FT–IR spectrum of amine–functionalized HBPSi macromonomer.

3.2.2 Molecular structure analysis of HBPSi

Main molecular structure parameters of HBPSi were illustrated in table 2 (The MALLS–SEC traces and Mark–Houwink–Sakurada plots of HBPSi were given in figure S1 of the Supplementary Information). As indicated, HBPSi macromonomers possessed a relatively narrow molecular weight distribution (M_w/M_n) of 1.352. The weight–average molecular weight (M_w) and hydrodynamic radius ($R_{h(n)}$) of HBPSi were 5173 g/mol and 0.7 nm, respectively. The amine content of HBPSi macromonomers was determined by using elemental analysis in CHN mode and was finally calculated to be ca. 0.47 mmol/g based on the nitrogen percentage. Combining with its molecular weight (M_n = 3826 g/mol, M_w = 5173 g/mol), the average number of –NH$_2$ units on each HBPSi molecule was estimated to be about 1.8 and 2.4, suggesting that, on average, HBPSi macromonomer possesses ca. two –NH$_2$ units on each molecule, which could meet our requirements and are capable of co–polymerizing with ODA and PMDA to fabricate HBPSi polyimides.

In order to study the compact conformation of HBPSi, its intrinsic viscosity, [η], was measured in THF at 25 °C by SEC, which is typically correlated with their molecular weight by the Mark–Houwink–Sakurada (MHS) equation:

$$[\eta] = KM^{\alpha} \tag{2}$$

where α, the MHS exponent, is a parameter corresponding to the topology of a polymer in a good solvent [41-42]. Generally, for hyperbranched polymers, the exponent typically varies from 0.5 to 0.2, depending on the degree of branching, whereas for a linear polymer in a good solvent, the MHS exponent is typically in the range of 0.6–0.8, suggesting its random coil conformation [42]. As table 2 indicated, the MHS exponent of HBPSi was 0.39, which is significantly lower than that of a linear polymer, suggesting HBPSi possesses hyperbranched architecture. However, during the condensation reactions of silanols, intramolecular cyclization is likely to occur. Thus it is reasonable that HBPSi macromonomer is possibly less perfect in structure than common dendrimers [41].

3.2.3 FT–IR spectra of HBPSi polyimides
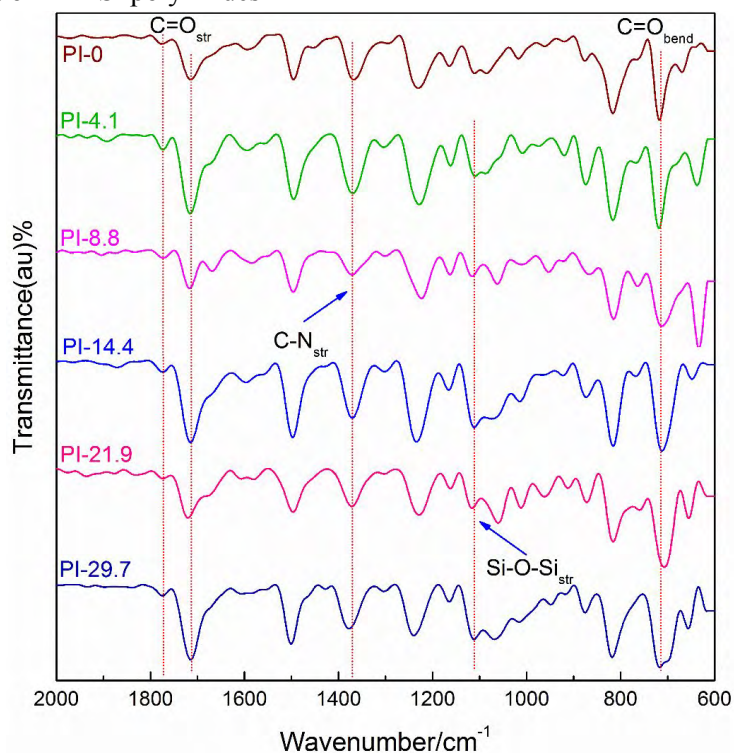
Figure 3. FT–IR spectra of resulting polyimides (Note: for convenience, *x* wt % HBPSi polyimide is

denoted as PI–*x*, similarly hereinafter).

Infrared spectra were measured for all membranes. As shown in figure 3, the appearance of characteristic imide group peaks at 1780 cm^{-1} (C=O asymmetrical stretching), 1715 cm^{-1} (C=O symmetrical stretching), 1375 cm^{-1} (C–N stretching) and 721 cm^{-1} (C=O bending), and the absence of the characteristic peaks of polyamic acid around 1650 cm^{-1} (C=O stretching of polyamic acid) and 1535 cm^{-1} (C–N stretching of polyamic acid) in FT–IR spectra indicated that imidization is complete. The characteristic absorption bands around 1100 cm^{-1} in the spectra suggested that Si–O–Si network was present in hybrid membranes [28].

3.3 Mechanical properties of polyimide membranes

Table 3. Intrinsic viscosities of polyamic acids and properties of resulting polyimide membranes.

| Sample	$\eta_{inh}{}^{a}$(dL·g^{-1})	Membrane density (g·cm^{-3})^{b}	Tensile strength (MPa)^{c}	Break elongation (%)^{c}
Pristine–PI	3.32	1.412	113.4	26
4.1 wt % HBPSi–PI	3.84	1.397	126.1	24
8.8 wt % HBPSi–PI	2.45	1.378	109.1	20
14.4 wt % HBPSi–PI	2.10	1.370	95.0	11
21.9 wt % HBPSi–PI	1.53	1.356	81.3	10
29.7 wt % HBPSi–PI	1.43	1.350	76.8	8

[a] Determined in DMAc (0.5 g·dL^{-1}) at 25 °C for polyamic acids. [b] Measured by liquid suspension method at ambient conditions. [c] Measured with a universal testing machine (UTM).

Table 3 illustrated the mechanical performances of the polyimide membranes. Tensile strengths and elongations at break of resulting membranes ranged from 76.8 to 126.1 MPa and 8 to 26%, respectively. For polyimide membranes, tensile strength mostly depends on molecular weight and packing density of molecular chains, whereas elongation at break generally on flexural nature or flexibility of molecular chains. As shown in table 3, intrinsic viscosities of formulated polyamic acids, except 4.1 wt % HBPSi PAA, gradually decrease with increasing HBPSi loading amount, suggesting a decreasing molecular weight of finally formed polyimides. Additionally, as demonstrated in table 3, the decreasing membrane density suggested an inefficient chain–chain packing. Thus the above two causes possibly resulted in decreasing tensile strength of polyimide membranes. On the other hand, HBPSi molecules might remarkably increase the stiffness and rigidity of polyimide chains. This might lead to a restricted rotational motion of polyimide segments and resulted in reduced elongations at break. Moreover, 4.1 wt % HBPSi PAA displayed the highest intrinsic viscosity, most likely a result of crosslinking effect afforded by multi amine groups on HBPSi molecules. This might account for its higher tensile strength and slightly lower break elongation in comparison to pristine polyimide.

3.4 Atomic oxygen resistance of resulting polyimides

Ground–based AO exposure measurements were performed on membrane samples by utilizing a neutral beam producing facility in our lab. The exposure area is a circular domain with a diameter of 30 mm and the thickness of membranes ranges from 35 to 45 μm. During AO exposure, all samples were handled in vacuum chamber and irradiated to various AO fluences ranging from 0.88 to 3.87 $\times$ 10^{20} O atoms·cm^{-2}. Exposure to 3.87 $\times$ 10^{20} O atoms·cm^{-2} Kapton–equivalent AO fluence is roughly equivalent to one year exposure in LEO environment [22]. The AO fluence was controlled by

irradiation duration and the fluence of each exposure test was monitored by using a witness sample Kapton® H, which is installed on the sample holder and exposed to AO under identical conditions. The fluence was finally calculated according to Eq. (1) by measuring the mass loss of Kapton® H. The specific results of AO exposure tests were presented in figure 4. As indicated, mass loss of polyimide membranes dramatically decreases with increasing HBPSi loading amount and this is more apparent at high AO fluence. For pristine polyimide, mass loss approximately exhibited as a linear function of total AO fluence throughout the whole exposure period, while mass loss of HBPSi polyimides exhibited as a nonlinear function and gently increased with AO fluence. Additionally, mass loss rate of hybrid membranes gradually decreased with increasing AO fluence, suggesting that hybrid membranes were becoming increasingly resistant to AO attack with AO fluence. For 29.7 wt % HBPSi polyimide, it exhibited a mass loss of ~13.3 % that of pristine polyimide after exposure to AO fluence of 0.88×10^{20} O atoms·cm^{-2}. More specifically, in an AO exposure with a total fluence of 3.87×10^{20} O atoms·cm^{-2}, mass loss was merely ~5.9% that of pristine polyimide. These results suggested that HBPSi molecules are of significant importance in resisting AO attack and impart high AO survivability to hybrid polyimides in the simulated AO environment. On the other hand, when HBPSi loading exceeds 8.8 wt %, such as PI–14.4, PI–21.9 and PI–29.7, mass loss of these samples seems quite small, demonstrating that only PI–14.4, PI–21.9 and PI–29.7 exhibited admirable AO resistance. The specific causes for this will be discussed later.
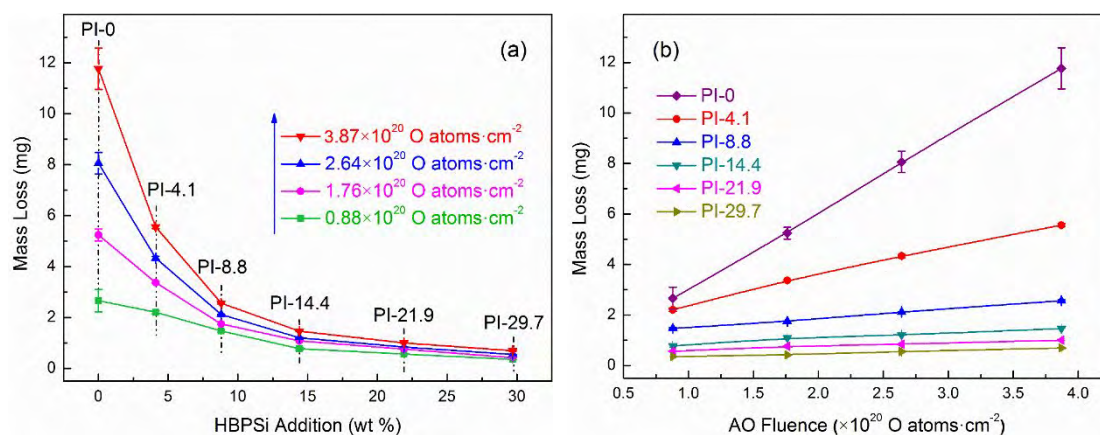

Figure 4. Mass loss of resulting polyimide membranes after exposure to various AO fluences: (a) mass loss vs HBPSi addition; (b) mass loss vs AO fluence.

X–ray Photoelectron Spectroscopy (XPS) measurements were adopted to detect changes in electron states and compositions of surface elements on topmost surface (approximately 0–10 nm) of the polyimide membranes. In the current investigation, all sample surfaces before and after exposure to various AO fluences have been probed by XPS and the results were illustrated in figure 5 and figure 6. For pristine polyimide, surface compositions changed insignificantly and only a slight decrease in carbon atomic concentration is visible. However, this is absolutely not the case for hybrid membranes. It is clearly indicated that, a significant decrease in carbon atomic concentration and a remarkable increase in oxygen atomic concentration were typically observed after exposure to neutral AO beam and, reduction of carbon atomic concentration seemed to appear a growing trend with increasing both AO fluence and HBPSi addition. Moreover, silicon atomic concentration of unexposed hybrid membranes was very low, only a few percent, but it presented a dramatical increase in all cases even after a small dose of AO irradiation, suggesting that surface atoms like carbon, hydrogen and nitrogen possibly generated off–gassing of volatile species (such as CO, CO_2, NO_x and HO_x), while silicon

atoms remained and were eventually oxidized to silicon oxides (SiO_x) when AO reacted with a hydrocarbon–based surface [6,19,23,24].
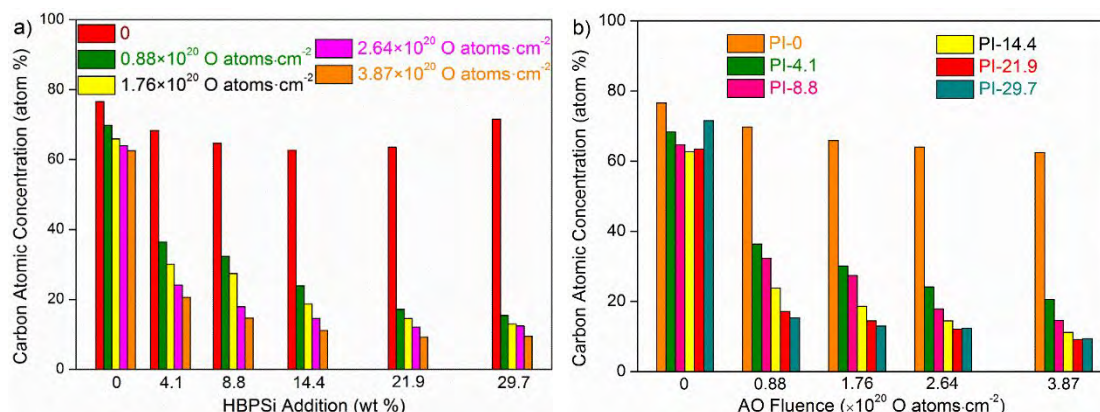

Figure 5. Surface atomic concentration of carbon (atom %) determined from XPS survey scans for HBPSi polyimide membranes after exposure to various AO fluences: (a) concentration vs HBPSi addition; (b) concentration vs AO fluence.
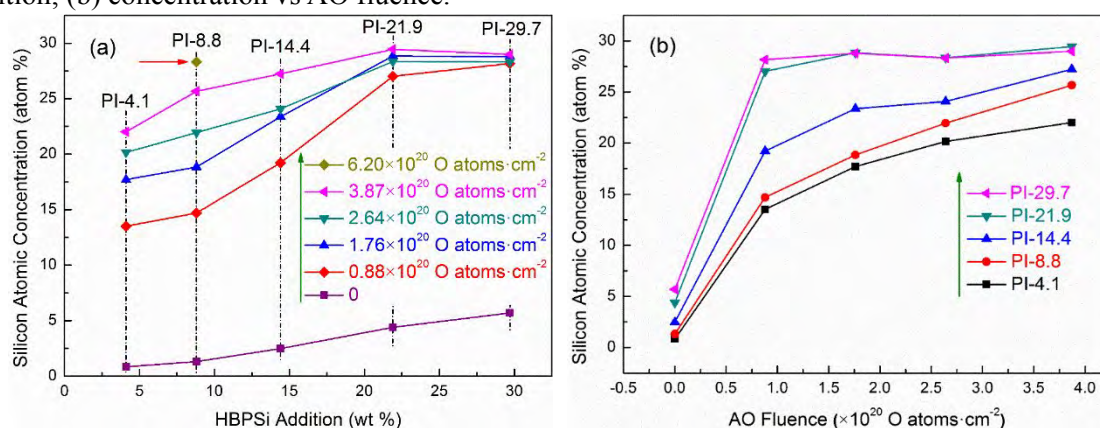

Figure 6. Surface atomic concentration of silicon (atom %) determined from XPS survey scans for HBPSi polyimide membranes after exposure to various AO fluences: (a) concentration vs HBPSi addition; (b) concentration vs AO fluence.

High–resolution XPS survey spectra of C 1s, O 1s and Si 2p peaks were obtained corresponding to all polyimide membranes before and after exposure to AO, and the Si 2p spectra of select samples, PI–4.1 and PI–29.7 are shown in figure 7. As indicated, peaks at ~101.3 eV and ~102 eV, possibly corresponding to suboxide and silsesquioxane (Si_2O_3) [23,24], became dramatically less pronounced while the intensity of peaks at higher binding energy significantly increased with increasing AO fluence. Additionally, the Si 2p peaks displayed an evident shift of ~1.7 eV from a lower binding energy of ~102 eV to ~103.7 eV, most likely from Si_2O_3 to SiO_2, indicating the AO had reacted with HBPSi molecules by O atom addition to Si–O and Si–C bonds followed by Si–C bonds scission [12,23,24], thus the HBPSi molecules had been disrupted and oxidized, ultimately to give silica. This hypothesis was also supported by the O/Si ratio shown in figure 8. When AO fluence increased from 0.88 to 3.87×10^{20} O atoms·cm^{-2}, O/Si ratio of hybrid membranes gradually tended towards 2/1 and this is much more apparent for polyimides with higher HBPSi addition. It is significant to note that O/Si ratio of PI–21.9 and PI–29.7 rapidly reached approximately 2/1 albeit undergoing a small dose of AO irradiation of 0.88×10^{20} O atoms·cm^{-2} and the ratio seems almost unaffected as AO fluence increases, implying a rapid conversion of silsesquioxane to SiO_2 upon AO exposure [29]. This is well consistent with remarkable decrease in their surface carbon atomic concentration illustrated in figure 5.

All these data suggested a protection mechanism that almost the entire polyimide portions on the topmost surface had been eroded away by the incoming AO and a passivating silica layer formed on the membrane surface, which is survivable in the AO environment and possibly plays the role of a protective coating and consequently leads to gentle mass loss as well as superior AO resistance [23,24,28].
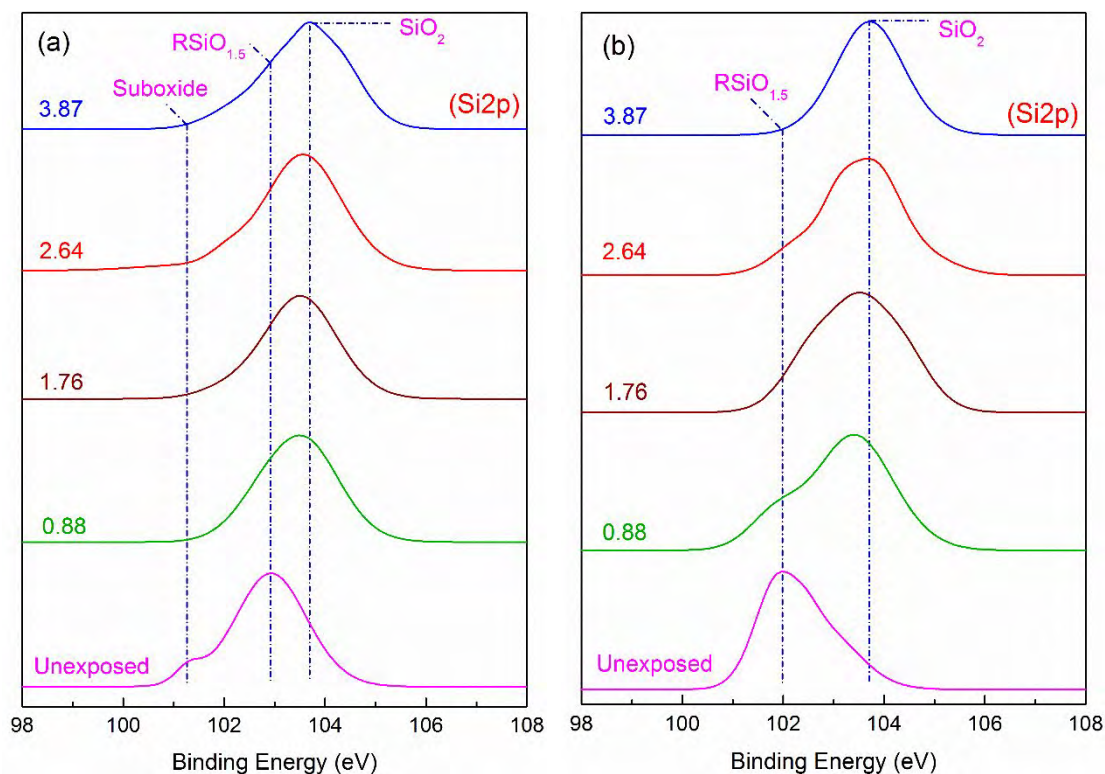
Figure 7. High–resolution XPS spectra of Si 2p curves corresponding to (a) 4.1 wt % HBPSi and (b) 29.7 wt % HBPSi polyimide membranes before and after exposure to various AO fluences of 0.88×10^{20} O atoms·cm^{-2}, 1.76×10^{20} O atoms·cm^{-2}, 2.64×10^{20} O atoms·cm^{-2} and 3.87×10^{20} O atoms·cm^{-2}.
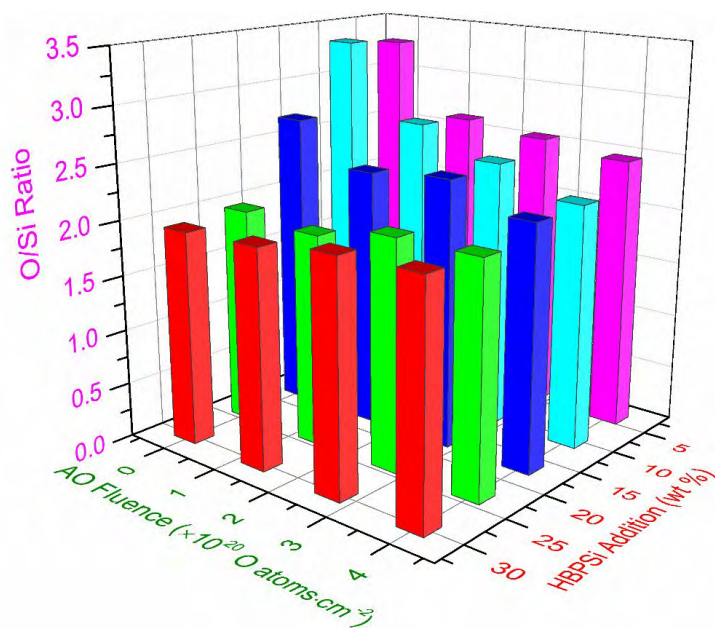
Figure 8. Three–dimensional diagram for O/Si ratio graphed in terms of the HBPSi addition and AO

fluence.

In order to understand the specific effects of the HBPSi molecules on AO reaction efficiency, the AO erosion yield was calculated according to Eq. (1) for all samples. The erosion yields of resulting membranes were graphed in figure 9 as the function of HBPSi addition and AO fluence. It is clearly seen that, the higher the HBPSi content of a sample or the larger the AO fluence, the smaller the erosion yield. Additionally, there appeared a significant reduction in AO erosion yield when the HBPSi loading surpasses 8.8 wt %, suggesting that polyimides with lower HBPSi addition are possibly insufficient to generate any significant enhancement to AO resistance towards AO attack. This is to say that there is a threshold of HBPSi addition to significantly enhance the AO resistance of HBPSi polyimides. There are a few possible causes for the significant reduction in mass loss and AO erosion yield for HBPSi polyimides. Since the surface coverage of organic moiety gradually decreases as HBPSi loading increases, this might result in smaller mass loss and enhanced AO resistance during AO irradiation. In addition, phenyl–substituted macromonomer HBPSi, might demonstrate slower degradation in the AO environment due to the admirable stability of benzene ring. However, these cannot possibly account for the entire significant reduction in mass loss and in AO erosion yield. As discussed above, upon AO exposure, the hydrocarbon–based moiety, namely, polyimide portion, is likely to be much more easily etched at the early stage. Simultaneously, silicon atoms are exposed on the membrane surface and are eventually oxidized to a self–organized SiO_2 passivating layer. As shown in figure 7, however, HBPSi polyimide with low or high HBPSi loading seems capable of forming this admirable protective layer to resist AO attack. Therefore, all HBPSi polyimide samples are likely to exhibit admirable AO resistance once the topmost polyimide portions have been completely etched during long–time AO exposure and no threshold of HBPSi addition appears. However, this is not the case. It is clearly indicated that, only when the HBPSi loading is sufficiently high, hybrid membranes such as PI–14.4, PI–21.9 and PI–29.7 could exhibit desirable AO resistance, as can be clearly observed from figure 4. In order to develop an understanding of the threshold, surface morphologies of all samples before and after exposure to various AO fluences were observed by using scanning electron microscope (SEM).
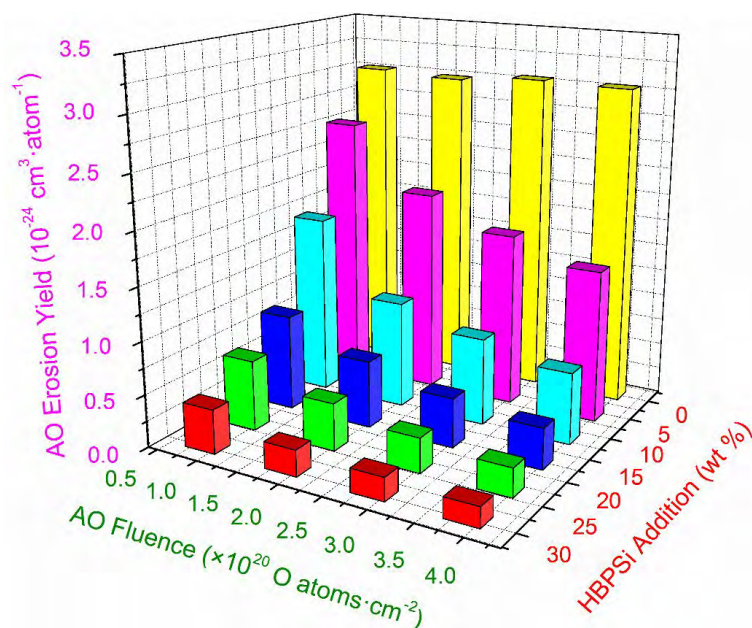

Figure 9. Three–dimensional diagram for AO erosion yield graphed in terms of the HBPSi addition

and AO fluence.

As shown in figure 10, prior to AO irradiation, the hybrid membranes presented flat and smooth surface morphologies. Nevertheless, surfaces of all samples had been significantly roughened with increasing AO fluence, and in particular PI−4.1, presented "carpet−like" morphology, which is similar to pristine polyimide as demonstrated in our previous study [28,29]. From PI−4.1 to PI−29.7, membrane surfaces became decreasing rough. For PI−29.7, the surface roughness turned to a much lower extent in comparison to pristine polyimide under the same conditions [28]. The superior AO resistance of polyimides containing HBPSi molecules is once again highlighted by their surface morphologies.

Prior to exposure 1.76×10^{20} **atoms·cm^{-2}** 3.87×10^{20} **O atoms·cm^{-2}**
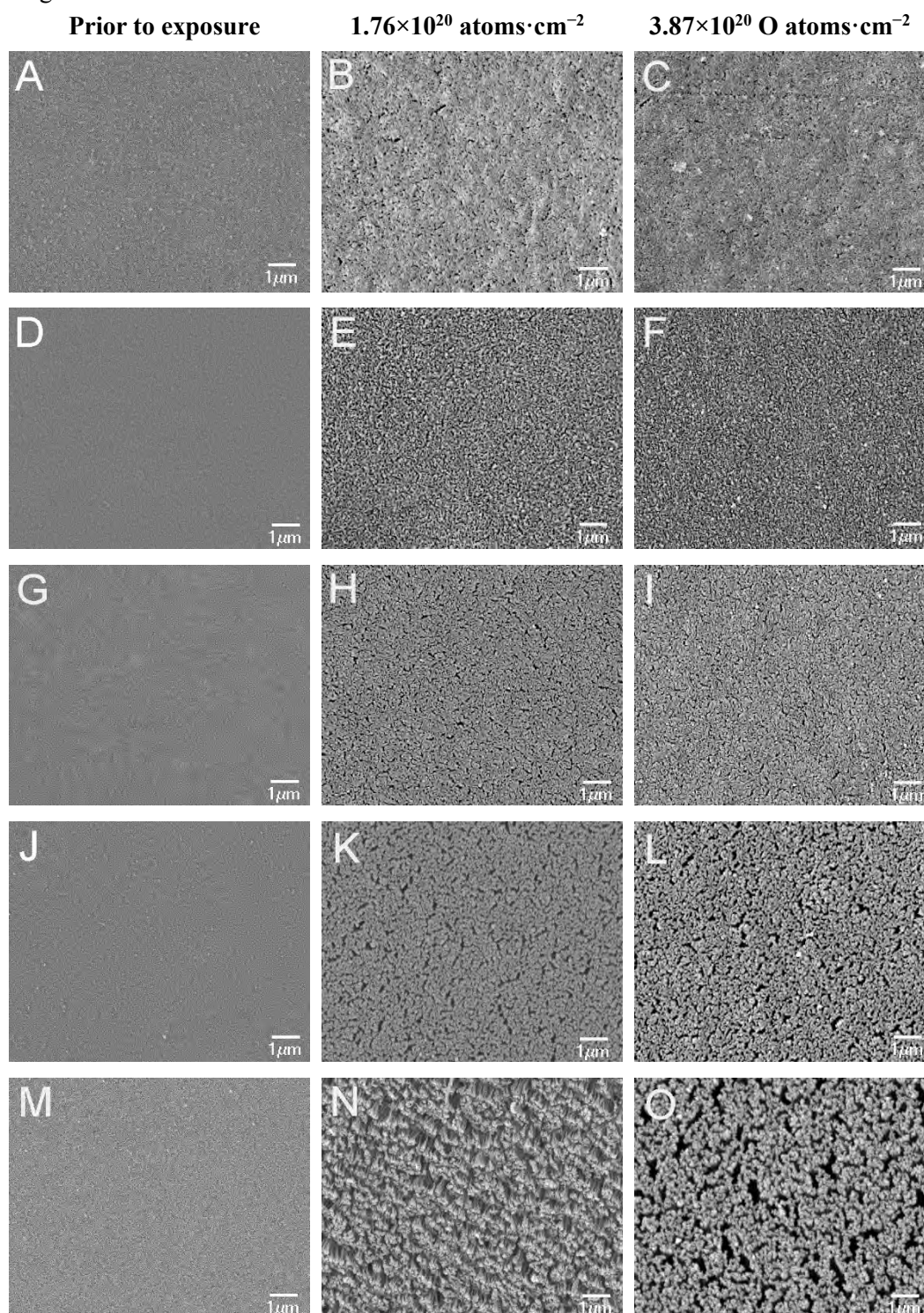
Figure 10. Select SEM images of HBPSi polyimide membranes: PI−29.7 (A−C); PI−21.9 (D−F); PI−14.4 (G−I); PI−8.8 (J−L) and PI−4.1 (M−O) before and after exposure to AO fluences of 1.76×10^{20} and 3.87×10^{20} O atoms·cm^{-2}. Note: AO fluence is shown above corresponding images and the scale bar at the bottom of each image indicates 1 μm.

As mentioned above, only when the HBPSi loading is sufficiently high, hybrid membranes could exhibit admirable AO survivability. It is interesting that this phenomenon once again emerges in surface morphologies as demonstrated in figure 10. Form PI−4.1 to PI−8.8, the surfaces had significantly roughened after exposure to AO and a few microcracks appeared, while for PI−14.4, PI−21.9 and PI−29.7, their surfaces were becoming increasing denser. As mentioned above, the "self−organized" silica passivating layer is crucial to prevent the "ambitious" AO from etching the underlying polyimide matrix. Therefore, it would make sense that samples exhibiting desirable AO resistance are likely to be covered with a much denser and more connected silica protective layer [6]. It is clearly indicated that, for PI−4.1 and PI−8.8, their surfaces are less dense than the others, testifying that the passivating layer is imperfect nor connected and thus is insufficient to protect the bulk polyimide matrix from AO attack. In fact, during the initial stages of oxidation of a HBPSi polyimide, erosion of the organic portions of hybrid polyimide occurs and will compete with the development of a SiO$_2$ passivating layer [6,28,29]. Thus when HBPSi loading is not sufficiently high, such as 4.1 wt %, polyimide erosion might be significant and make a dominated contribution to mass loss. However, when HBPSi content exceeds 8.8 wt %, more HBPSi molecules might be involved in this competition and, as a consequence, the silica passivating layer possibly formed within shorter time and could effectively resist AO attack, finally leading to superior AO resistance and smoother surface morphology. On the other hand, the silica passivating layer is likely to tend perfect with increasing AO fluence, for more Si−C bonds might be cleaved by incoming AO and oxidized to SiO$_2$ [24]. This is also supported by the surface morphologies illustrated in figure 10. As a result, as shown in figure 4(b), the mass loss rate of HBPSi polyimides gradually decreased and mass loss curves exhibited as a nonlinear function of AO fluence.

4. Conclusions

A novel amine−functionalized polysiloxane (HBPSi) with hyperbranched architecture was synthesized and characterized. A facile method to fabricate space survivable polyimide membranes with covalently bonded HBPSi is described. The resulting HBPSi polyimides exhibited a combination of desirable properties, especially superior AO survivability. With several surface analytical techniques, the resistance of resulting HBPSi polyimides to AO attack in a ground−based simulated LEO environment has been systematically investigated. The results indicated that HBPSi polyimides formed a silica passivating layer, which largely resisted AO attack and exhibited the lowest AO erosion yield of $\sim 1.9 \times 10^{-25}$ cm^3·atom^{-1}, approximately two orders of magnitude reduction that of the pristine polyimide. Moreover, only when the HBPSi loading is sufficiently high, the hybrid polyimides could exhibit admirable AO resistance, implying a threshold of HBPSi loading. XPS analysis revealed a protection mechanism that the organic polyimide portions were eroded away upon AO exposure and silicon were oxidized and finally generated a SiO$_2$ passivating layer. SEM images indicated that surfaces of HBPSi polyimide membranes tended to be increasing denser and smoother with increasing both HBPSi amount and AO fluence. Moreover, a dense and connected passivating layer plays a more positive role in resisting AO attack upon AO exposure and this might be mainly responsible for the threshold of HBPSi addition. The silica passivating layer limited the AO erosion yield to a fairly low value, this promises HBPSi polyimide membranes may find potential usage as surface protective

materials onboard spacecrafts to resist AO attack in the LEO environment.

Author information

*Corresponding Author, E–mail: qyzhang@nwpu.edu.cn; Tel: +86–029–88431675; Fax: +86–029–88431653.

Acknowledgements

Reference

[1] Zhao, X. H.; Shen, Z. G.; Xing, Y. S.; Ma, S. L. *J. Phys. D: Appl. Phys.* **2001**, 34, 2308–2314.

[2] Fischer, H. R.; Tempelaars, K.; Kerpershoek, A.; Dingemans, T.; Iqbal, M.; Lonkhuyzen, H. V.; Iwanowsky, B.; Semprimoschnig, C. *ACS Appl. Mater. Interfaces* **2010**, 2, 2218–2225.

[3] Gouzman, I.; Girshevitz, O.; Grossman, E.; Eliaz, N.; Sukenik, C. N. *ACS Appl. Mater. Interfaces* **2010**, 2, 1835–1843.

[4] Bedingfield, K. L.; Leach, R. D.; Alexander, M. B. Spacecraft System Failures and Anomalies Attributed to the Natural Space Environment; NASA Reference Publication 1390; National Aeronautics and Space Administration: Washington, D.C., 1996.

[5] Minton, T. K.; Garton, D. J. Dynamics of Atomic–Oxygen–Induced Polymer Degradation in Low Earth Orbit. In Chemical Dynamics in Extreme Environments; Dressler, R. A., Ed; Advanced Series in Physical Chemistry; World Scientific: Singapore, 2001; pp 420–489.

[6] Minton, T. K.; Wright, M. E.; Tomczak, S. J.; Marquez, S. A.; Shen, L. H.; Brunsvold, A. L.; Cooper, R.; Zhang, J. M.; Vij, V.; Guenthner, A. J.; Petteys, B. J. *ACS Appl. Mater. Interfaces* **2012**, 4, 492–502.

[7] Leger, L. J.; Visentine, J. T. *J. Spacecr. Rockets* **1986**, 23, 505–511.

[8] He, L.; Wagner, S. R.; Illingsworth, M. L.*Chem. Mater.* **1997**, 9, 3005–3011.

[9] Tagawa, M.; Yokota, K.; Kishida, K.; Okamoto, A.; Minton, T. K. *ACS Appl. Mater. Interfaces* **2010**, 2, 1866–1871.

[10] Minton, T. K.; Wu, B.; Zhang, J.; Lindholm, N. F.; Abdulagatov, A. I.; O'Patchen, J.; George, S. M.; Groner, M. D. *ACS Appl. Mater. Interfaces* **2010**, 2, 2515–2520.

[11] Shpilman, Z.; Gouzman, I.; Grossman, E.; Shen, L.; Minton, T. K.; Paci, J. T.; Schatz, G. C.; Akhvlediani, R.; Hoffman, A. *J. Phys. Chem. C* **2010**, 114, 18996–19003.

[12] Miyazaki, E.; Tagawa, M.; Yokota, K.; Yokota, R.; Kimoto, Y.; Ishizawa, J. *Acta Astronaut.* **2010**, 66, 922–928.

[13] Fong, H.; Vaia, R. A.; Sanders, J. H.; Lincoln, D.; Vreugdenhil, A. J.; Liu, W.; Bultman, J.; Chen, C. *Chem. Mater.* **2001**, 13, 4123–4129.

[14] Tagawa, M.; Maeda, K. I.; Kajita, T.; Yokota, K.; Akamatsu, K.; Nawafune, H. *Langmuir* **2007**, 23, 11351–11354.

[15] Murad, E. *J. Spacecr. Rockets* **1996**, 33, 131–136.

[16] Reddy, M. R. *J. Mater. Sci.* **1995**, 30, 281–307.

[17] Vanherck, K.; Vandezande, P.; Aldea, S. O.; Vankelecom, I. F. J. *J. Membrane Sci.* **2008**, 320, 468–476.

[18] Koshikawa, H.; Usui, H.; Maekawa, Y. *J. Membrane Sci.* **2009**, 327, 182–187.

［19］Verker, R.; Grossman, E.; Gouzman, I.; Eliaz, N. *High Perform. Polym.* **2008**, 20, 475–491.

［20］Ba, C.; Economy, J. *J. Membrane Sci.* **2010**, 363, 140–148.

［21］Gouzman, I.; Grossman, E.; Lempert, G.; Noter, Y.; Altshuler, Y.; Lifshitz, Y. *High Perform. Polym.* **2001**, 13, S505–S516.

［22］Watson, K. A.; Palmieri, F. L.; Connell, J. W. *Macromolecules* **2002**, 35, 4968–4974.

［23］Tomczak, S. J.; Marchant, D.; Svejda, S.; Minton, T. K.; Brunsvold, A. L.; Gouzman, I.; Grossman, E.; Schatz, G. C.; Troya, D.; Sun, L. P.; Gonzalez, R. I. *Mater. Res. Soc. Symp. Proc.* **2005**, 851, NN9.1.1–NN9.1.12.

［24］Brunsvold, A. L.; Minton, T. K.; Gouzman, I.; Grossman, E.; Gonzalez, R. *High Perform. Polym.* **2004**, 16, 303–318.

［25］Gonzalez, R. I.; Phillips, S. H. *J. Spacecr. Rockets* **2000**, 37, 463–467.

［26］Devapal, D.; Packirisamy, S.; Korulla, R. M.; Ninan, K. N. *J. Appl. Polym. Sci.* **2004**, 94, 2368–2375.

［27］Yokota, K.; Abe, S.; Tagawa, M.; Iwata, M.; Miyazaki, E.; Ishizawa, J. I.; Kimoto, Y.; Yokota, R. *High Perform. Polym.* **2010**, 22, 237–251.

［28］Lei X. F.; Chen Y.; Zhang H. P.; Li, X. J.; Yao, P.; Sun, W. L.; Zhang, Q. Y. *ACS Appl. Mater. Interfaces* **2013**, 5, 10207–10220.

［29］Lei, X. F.; Yao, P.; Qiao, M. T.; Sun, W. L.; Zhang, H. P.; Zhang, Q. Y. *High Perform. Polym.* **2014**, DOI: 10.1177/0954008314528011.

［30］Tanaka, K.; Chujo, Y. *J. Mater. Chem.* **2012**, 22, 1733–1746.

［31］Choi, J.; Tamaki, R.; Kim, S. G.; Laine, R. M. *Chem. Mater.* **2003**, 15, 3365–3375.

［32］Zhang, X.; Ren, H.; Wang, J.; Zhang, Y.; Shao, Y. *Mater. Lett.* **2011**, 65, 821–824.

［33］Sakka, S.; Tanaka, Y.; Kokubo, T. *J. Non–Cryst. Solids* **1986**, 82, 24–30.

［34］Hualee, L.; Chen, W. C.; Liu, W. C. *J. Polym. Sci., Part A: Polym. Chem.* **2002**, 40, 1560–1571.

［35］Dworak, D. P.; Soucek, M. D. *Macromol. Chem. Phys.* **2006**, 207, 1220–1232.

［36］Hook, R. J. *J. Non–Cryst. Solids* **1996**, 195, 1–15.

［37］Tsai, M. F.; Lee, Y. D.; Chen, K. N. *J. Appl. Polym. Sci.* **2002**, 86, 468–477.

［38］Prabakar, S.; Assink, R. A.; Raman, N. K.; Myers, S. A.; Brinker, C. J. *J. Non–Cryst. Solids* **1996**, 202, 53–60.

［39］Nair, B. P.; Pavithran, C. *Langmuir* **2010**, 26, 730–735.

［40］Huang, J. C.; He, C. B.; Xiao, Y.; Mya, K. Y.; Dai, J.; Siow, Y. P. *Polymer* **2003**, 44, 4491–4499.

［41］Chen, H.; Kong, J.; Tian, W.; Fan, X. D. *Macromolecules* **2012**, 45, 6185–6195.

［42］Kong, J.; Schmalz, T.; Motz, G.; Müller, A. H. E. *Macromolecules* **2011**, 44, 1280–1291.

End of Lecture